Neurobiology of Disease 178 (2023) 106020

Contents lists available at ScienceDirect

Neurobiology of Disease

journal homepage: www.elsevier.com/locate/ynbdi

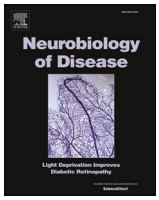

Pharmacological inhibition of lysosomal two-pore channel 2 (TPC2) confers neuroprotection in stroke via autophagy regulation

Valentina Tedeschi [a], Antonio Vinciguerra [b], Maria Josè Sisalli [a], Giuseppe Pignataro [a], Agnese Secondo [a,*]

[a] Division of Pharmacology, Department of Neuroscience, Reproductive and Odontostomatological Sciences, School of Medicine, "Federico II" University of Naples, Via Sergio Pansini 5, Naples 80131, Italy
[b] Department of Biomedical Sciences and Public Health, School of Medicine, University "Politecnica delle Marche", Via Tronto 10/A, Ancona 60126, Italy

ARTICLE INFO

Keywords:
TPC2
Lysosomal function
Autophagy
Focal ischemia
Hypoxia
ER stress

ABSTRACT

Lysosomal function and organellar Ca^{2+} homeostasis become dysfunctional in Stroke causing disturbances in autophagy, the major process for the degradation of abnormal protein aggregates and dysfunctional organelles. However, the role of autophagy in Stroke is controversial since excessive or prolonged autophagy activation exacerbates ischemic brain injury. Of note, glutamate evokes NAADP-dependent Ca^{2+} release via lysosomal TPC2 channels thus controlling basal autophagy. Considering the massive release of excitotoxins in Stroke, autophagic flux becomes uncontrolled with abnormal formation of autophagosomes causing, in turn, disruption of excitotoxins clearance and neurodegeneration. Here, a fine regulation of autophagy via a proper pharmacological modulation of lysosomal TPC2 channel has been tested in preclinical Stroke models. Primary cortical neurons were subjected to oxygen and glucose deprivation+reoxygenation to reproduce in vitro brain ischemia. Focal brain ischemia was induced in rats by transient middle cerebral artery occlusion (tMCAO). Under these conditions, TPC2 protein expression as well as autophagy and endoplasmic reticulum (ER) stress markers were studied by Western blotting, while TPC2 localization and activity were measured by immunocytochemistry and single-cell video-imaging, respectively. TPC2 protein expression and immunosignal were highly modulated in primary cortical neurons exposed to extreme hypoxic conditions causing dysfunction in organellar Ca^{2+} homeostasis, ER stress and autophagy-induced cell death. TPC2 knocking down and pharmacological inhibition by Ned-19 during hypoxia induced neuroprotection. The effect of Ned-19 was reversed by the permeable form of TPC2 endogenous agonist, NAADP-AM. Of note, Ned-19 prevented ER stress, as measured by GRP78 (78 kDa glucose-regulated protein) protein reduction and caspase 9 downregulation. In this way Ned-19 restored organellar Ca^{2+} level. Interestingly, Ned-19 reduced the infarct volume and neurological deficits in rats subjected to tMCAO and prevented hypoxia-induced cell death by blocking autophagic flux. Collectively, the pharmacological inhibition of TPC2 lysosomal channel by Ned-19 protects from focal ischemia by hampering a hyperfunctional autophagy.

1. Introduction

Autophagy is a lysosome-dependent clearing process that may represent a gatekeeping mechanism for stabilizing cellular homeostasis in Stroke (Li et al., 2014; Zuo et al., 2014; Yu et al., 2016). In fact, lysosomal function becomes dysfunctional in Stroke (Zhang et al., 2020) as well as in various neurological diseases representing a potential neuroprotective target (Tedeschi et al., 2019a; Udayar et al., 2022). Mutations in several genes involved in the global lysosomal network have been causatively linked to the neurodegenerative process (Nixon, 2013; Colacurcio and Nixon, 2016). Moreover, the role of autophagy in Stroke is under rigorous evaluation; while increasing evidence support the protective role of autophagy in neuronal cells subjected to ischemia, excessive or prolonged autophagy activation may exacerbate ischemic brain injury inducing neuronal necroptosis and apoptosis (Hou et al., 2019; Zhang et al., 2021). Therefore, a fine control of this cleansing process is auspicable to exert neuroprotection. Moreover, defects in the lysosomal ionic machinery have been reported in several models of

* Corresponding author.
E-mail addresses: valentina.tedeschi@unina.it (V. Tedeschi), a.vinciguerra@univpm.it (A. Vinciguerra), mariajose.sisalli@unina.it (M.J. Sisalli), gpignata@unina.it (G. Pignataro), secondo@unina.it (A. Secondo).

https://doi.org/10.1016/j.nbd.2023.106020
Received 6 October 2022; Received in revised form 29 December 2022; Accepted 24 January 2023
Available online 26 January 2023
0969-9961/© 2023 The Authors. Published by Elsevier Inc. This is an open access article under the CC BY license (http://creativecommons.org/licenses/by/4.0/).

brain ischemia thus suggesting the relevant role of this tiny organelle as a hub of autophagy control (Zhang et al., 2020). Consistently, lysosome is now considered a relevant intracellular Ca^{2+} store provided of an its own machinery that is useful for the maintenance of local and general Ca^{2+} homeostasis. Recently, deregulation of Ca^{2+} signaling and lysosomal channel activity has been reported to occur in experimental models of Stroke (Tedeschi et al., 2021).

Lysosomal non-selective cation channels comprise the mucolipins (TRPML1–3) and two-pore channels (TPC1–2) implicated in neural development and function, and pathological processes. For instance, neuronal TRPML1 plays a crucial role in the regulation of lysosomal functions and autophagy (Medina et al., 2015), while its alteration may cause impairment of those cell pathways underlying neurodegeneration (Zhang et al., 2017; Tedeschi et al., 2019b; Santoni et al., 2020). Accordingly, in the neurodegenerative process, endogenous TRPML1 becomes defective contributing to the lysosomal Ca^{2+}-dependent alteration of autophagy (Bae et al., 2014; Tedeschi et al., 2019a and b; Santoni et al., 2020; Tsunemi et al., 2019). In contrast, hampering lysosomal and ER Ca^{2+} leak during ischemic preconditioning, the downregulation of TRPML1 lysosomal channel could be considered a newly identified neuroprotective mechanism in stroke (Tedeschi et al., 2021).

Lysosomal TPC2 is an ancient member of the voltage-gated ion channel superfamily (Patel, 2015) regulating the trafficking of various cargoes (Ruas et al., 2010; Grimm et al., 2014; Sakurai et al., 2015). Loss- and gain-of-function of TPCs are implicated in several neurodegenerative diseases (Patel, 2015; Patel and Kilpatrick, 2018). TPCs are considered non-selective Ca^{2+}-permeable channels when activated by NAADP (Grimm et al., 2014; Brailoiu et al., 2009; Calcraft et al., 2009; Brailoiu et al., 2010; Pitt et al., 2010; Schieder et al., 2010; Ruas et al., 2015) or highly-selective Na^{+} channels when stimulated by the endogenous agonist of TRPML1, $PI(3,5)P_2$, and/or voltage changes (Wang et al., 2012; Boccaccio et al., 2014; Cang et al., 2014; Guo et al., 2017; She et al., 2018).

NAADP-mediated release of Ca^{2+} from acidic stores through TPC2 regulates neuronal differentiation (Brailoiu et al., 2006), neurogenesis (Zhang et al., 2013), and axiogenesis in *Zebrafish* motor neurons (Guo et al., 2020). Neuronal stimulation by glutamate evokes NAADP synthesis and Ca^{2+} release from acidic stores through TPC channels (Foster et al., 2018; Hermann et al., 2020). Furthermore, several studies underpin the role of TPC2-mediated Ca^{2+} efflux in the modulation of basal autophagy (Pereira et al., 2011; Medina, 2021). Under conditions of severe energy depletion, TPC2 is involved in cell viability control by regulating autophagic flux in cardiomyocytes (García-Rúa et al., 2016). Moreover, glutamate stimulates autophagy via NAADP/TPC/AMPK pathway, thus controlling cell metabolism in the central nervous system (CNS) (Pereira et al., 2017).

Therefore, considering the massive and uncontrolled release of detrimental glutamate level during hypoxia, the regulation of the autophagic flux may result dysfunctional during Stroke. On the other hand, the abnormal formation of autophagosomes (Zhang et al., 2021) may disrupt the clearance of excitotoxins in Stroke (Katsumata et al., 2010). Therefore, hampering the autophagic flux through TPC2 modulation might constitute an innovative approach in Stroke therapy. In this study, we explored this avenue by studying the effect of TPC2 inhibition on neuronal survival under hypoxic conditions and the enlargement of infarct volume in rats subjected to focal ischemia. We showed that TPC2 pharmacological blockade by Ned-19 prevented autophagy-induced cell death in cortical cultures exposed to hypoxic conditions and reduced the extension of ischemic volume in rats subjected to tMCAO.

2. Materials and methods

2.1. Reagents

Primary antibodies used in this study are listed in Supplemental Table I. ECL reagents and nitrocellulose membranes were from GE Healthcare (Milan, Italy). Small interfering RNAs (siRNAs) and siRNA-control were purchased from Qiagen (Milan, Italy). GPN was purchased from Santa Cruz Biotechnology, Inc. (Dallas, TX, USA); *trans*-Ned-19 (Ned-19) was from Tocris Bioscience (Bristol, UK); NAADP-AM was from AAT Bioquest (Sunnyvale, CA, USA); ML-SA1 was from Merck Millipore (Darmstadt, Germany). Thapsigargin and MTT were from Sigma-Aldrich (Milan, Italy). 1-[2-(5-Carboxyoxazol-2-yl)-6-aminobenzofuran-5-oxy]-2-(21-amino-51-methylphenoxy)-ethane-N,N,N1, N1-tetraacetic acid penta-acetoxymethyl ester(Fura-2/AM) was from Molecular Probes (Life Technologies, Milan, Italy).

2.2. Cell cultures and siRNA transfection

Primary cortical neurons were obtained from brains of 14/16-day-old Wistar rat embryos, dissected and cultured as previously reported (Sirabella et al., 2009; Sisalli et al., 2014; Secondo et al., 2019). After 5–6 days in vitro, neurons were transfected with two different FlexiTube small interfering RNAs (siRNAs) against the lysosomal channel TPC2 (#1: #SI01704759, target sequence: TTCCGAGGCTACCTAATGAAA; #4: #SI01704780, target sequence: CCCGTGGTCGATGGTGTATTT) and with the non-targeting control (Qiagen, Milan, Italy). All the animal procedures were performed in accordance with the regulation 2010/63 from EU, the D.Lgs. 2014/26 from Italian Ministry of Health, and the experimental protocols was approved by OPBA of the "Federico II" University of Naples, Italy.

Human neuroblastoma SH-SY5Y cells were grown in DMEM supplemented with 10% FBS, 2 mM L-glutamine, 100 IU/ml penicillin and 100 μg/ml streptomycin.

2.3. Combined oxygen and glucose deprivation and reoxygenation

Hypoxic conditions were reproduced in vitro by exposing cortical neurons to oxygen and glucose deprivation (OGD) followed by reoxygenation (Rx), as previously reported (Sisalli et al., 2014). Briefly, the OGD was achieved by incubating neurons for 3 h in a glucose-free medium previously saturated with 95% N_2 and 5% CO_2 for 20 min and containing 116 mM NaCl, 5.4 mM KCl, 0.8 mM $MgSO_4$, 26.2 mM $NaHCO_3$, 1 mM NaH_2PO_4, 1.8 mM $CaCl_2$, 0.01 mM glycine and 0.001 *w/v* phenol red. A hypoxia chamber was used to keep neurons under hypoxic conditions (atmosphere 5% CO_2 and 95% N_2, temperature 37 °C). At the end of the incubation, the OGD was stopped by replacing the glucose-free medium with a culture medium containing normal levels of glucose and the reoxygenation was achieved by returning neurons to normoxic conditions (5% CO_2 and 95% air, temperature 37 °C) for 24 h.

2.4. Transient focal ischemia

After exposure to a mixture of 2% sevoflurane and 98% O_2 (Oxygen Concentrator Mod. LFY-I-5) Sprague Dawley male rats (Charles River, Italy) were subjected to transient focal ischemia (tMCAO) by suture occlusion of MCA for 100 min, as previously reported (Secondo et al., 2019). Achievement of ischemia was confirmed by monitoring regional cerebral blood flow through laser Doppler (PF5001; Perimed, Sweden). Animals not showing cerebral blood flow reduction of at least 70% ($N = 6$), as well as those dying after ischemia induction ($N = 5$), were excluded from the study. For the experiments, animals were divided into 5 experimental groups: (1) sham-operated rats, (2) ischemic rats treated with vehicle (tMCAO+vehicle), (3) ischemic rats treated with Ned-19 20× (0,6 mM) (tMCAO+Ned-19 20×), (4) ischemic rats treated with Ned19 40× (1,2 mM) (tMCAO+Ned-19 40×) and (5) ischemic rats treated with Ned-19 80× (2,4 mM) (tMCAO+Ned-19 80×). Ned-19 was intracerebroventricularly infused at the onset of reperfusion. The needle was left for an additional 5 min after the injection. Vehicle group was injected as Ned-19. Rectal temperature was maintained at 37 ± 5 °C

with a thermostatically controlled heating pad; arterial blood gases before and after ischemia were measured by a catheter inserted into the femoral artery (Rapid Laboratory 860, Chiron Diagnostic). Experiments were performed in a blinded manner. The animal study was approved by OPBA of the "Federico II" University of Naples, Italy, and by the Committee set by the Ministry of Health at the National Institute of Health (Rome). Animal handling was done in accordance with the ARRIVE international guidelines, minimizing animal suffering and reducing the number of animals.

2.5. Evaluation of neurological scores and ischemic volume

Neurological scores were evaluated at 24 h from tMCAO, immediately before the sacrifice, whereas the ischemic volume was evaluated with 2,3,5-triphenyl tetrazolium chloride staining 24 h after ischemia (Bederson et al., 1986; Vinciguerra et al., 2014).

2.6. Western blotting and co-immunoprecipitation

Total proteins were separated by SDS-PAGE gel electrophoresis and then electrotransferred onto 0.2 μm nitrocellulose membranes. For co-immunoprecipitation experiments, 500 μg of total protein extracts were immunoprecipitated.

2.7. Immunocytochemistry and confocal microscopy

Neurons were washed twice in cold PBS (pH 7.4) and fixed at room temperature in 4% paraformaldehyde for 20 min. Then, neurons were blocked in PBS containing 3% BSA for 30 min and then incubated overnight at 4 °C with anti-TPC2 and anti-LAMP1 antibodies. Control for the specificity of the antibody against TPC2 was performed with its replacement with normal serum as previously described (Tedeschi et al., 2019b; Secondo et al., 2019). Then, cells were washed with PBS and incubated with anti-rabbit Cy2-conjugated antibody or anti-mouse Cy3-conjugated antibody (Jackson Immuno Research Laboratories, Inc. PA, USA) for 1 h at RT under dark conditions. Cells were finally incubated with Hoechst. Cover glasses were mounted with a SlowFadeTM Antifade Kit (Molecular Probes, Life Technologies, Milan, Italy) and acquired by a 63× oil immersion objective using a Zeiss inverted 700 confocal microscope (Scorziello et al., 2013).

2.8. $[Ca^{2+}]_i$ measurements in single living cells

$[Ca^{2+}]_i$ was detected by single-cell Fura-2/AM computer assisted video-imaging (Secondo et al., 2007; Tedeschi et al., 2021). Results are presented as cytosolic Ca^{2+} concentration calculated by the equation of Grynkiewicz et al. (Grynkiewicz et al., 1985; Urbanczyk et al., 2006).

2.9. Cell viability

2.9.1. MTT assay

Cell viability was assessed as mitochondrial activity by the MTT (3 [4,5-dimethylthiazol-2-yl]-2,5-diphenyl-tetrazolium bromide) assay, as previously reported (Secondo et al., 2007). Briefly, after treatments, neurons were incubated with a 0.5 mg/mL MTT solution at 37 °C for 1 h. Then, samples were collected in dimethyl sulfoxide (DMSO) and, after the insoluble formazan crystals had dissolved, the absorbance was determined spectrophotometrically at 540 nm. The data were expressed as a percentage of cell viability compared to control cultures.

2.9.2. Lactate dehydrogenase (LDH) release assay

LDH release has been measured using the Cytotoxicity LDH assay Kit-WST (Dojindo, Kumamoto, Japan) according to the manufacturer's instructions. Cytotoxicity was calculated as a percentage of the ratio of LDH released in the extracellular medium compared to intracellular LDH released after cell lysis.

2.10. Detection of autolysosomes formation in live cells

The autolysosomes formation in live cells has been evaluated using the DALGreen – Autophagy Detection probe (Dojindo, Kumamoto, Japan), according to the manufacturer's protocol. In brief, cortical neurons plated on glass coverslips were incubated with 1 μmol/L DALGreen working solution at 37 °C for 24 h; for neurons exposed to OGD/Rx or OGD/Rx(+Ned-19), the probe was incubated at the onset of the reoxygenation phase for 21 h. Fluorescence images were acquired using a Zeiss Axiovert 200 microscope (Carl Zeiss, Germany), equipped with a MicroMax 512BFT cooled CCD camera (Princeton Instruments, Trenton, NJ, USA) (excitation wavelength: 485 nm). Image acquisition and processing were performed equally for all the experimental conditions by MetaMorph/MetaFluor Imaging System software (Universal Imaging). For the quantification of the fluorescent signal, background fluorescence was subtracted from the data.

2.11. Statistical analysis

Data are expressed as mean ± S.E.M. Statistical analysis was performed with one-way analysis of variance followed by Newman-Keuls test. Neurologic deficits were analyzed by the nonparametric Kruskal–Wallis test, followed by the Nemenyi test for the nonparametric multiple comparison. Differences were considered statistically significant when the p-value was <0.05.

3. Results

3.1. Characterization of neuronal TPC2 lysosomal channel in primary cortical neurons exposed to hypoxic conditions

Lysosomes are acidic organelles containing a high Ca^{2+} content and a low luminal pH. With the aim to characterize the role of TPC2 in cortical neurons under normoxic and hypoxic conditions, we performed immunocytochemistry and single-cell video-imaging together with mitochondrial viability measurement in the presence of the pharmacological inhibitor Ned-19. Under normoxia, TPC2 immunosignal was distributed within the soma and along the neuronal processes of rat primary cortical neurons and specifically co-localized with the lysosomal marker LAMP1 (Fig. 1A). The same subcellular distribution was detected in human SH-SY5Y cells (Fig. IA). The addition of the permeable form of NAADP (NAADP-AM,1 μM) induced a rapid Ca^{2+} release from TPC2 lysosomal channel that was blocked by the specific antagonist Ned-19 (30 μM) (Fig. 1B). However, the exposure to low oxygen level determined a huge reduction of TPC2 immunosignal during OGD while the exposure to reoxygenation induced an increased and diffused TPC2 immunolocalization (Fig. 1C). The same trend has been revealed by Western blotting depicting a significant downregulation of TPC2 protein expression in OGD and an increased expression under reoxygenation (Fig. 1D a,b). The specific inhibitor of TPC2, Ned-19 (30 μM), was able to prevent cell death in hypoxic neurons exposed to OGD + reoxygenation (Fig. 1E). This neuroprotective effect occurred exclusively when the drug was added during reoxygenation but not if administrated during OGD (Fig. 1E). Specifically, Ned-19 protected hypoxic neurons when it was added until 3 h of reoxygenation (Fig. I). This neuroprotective entity was similar to that produced by ischemic tolerance induced by an ischemic preconditioning stimulus (Fig. 1E) (Secondo et al., 2019). Moreover, in the presence of the permeable form of NAADP (NAADP-AM), Ned-19 failed to protect neurons from OGD+ reoxygenation thus highlighting the specificity of TPC2 role in neuroprotection (Fig. 1E). Of note, NAADP alone triggered the initiators of autophagy (i.e. LC3-II and Beclin-1) while reduced p62 protein expression after a brief exposure (Fig. II), thus showing the triggering role of TPC2 in autophagy regulation.

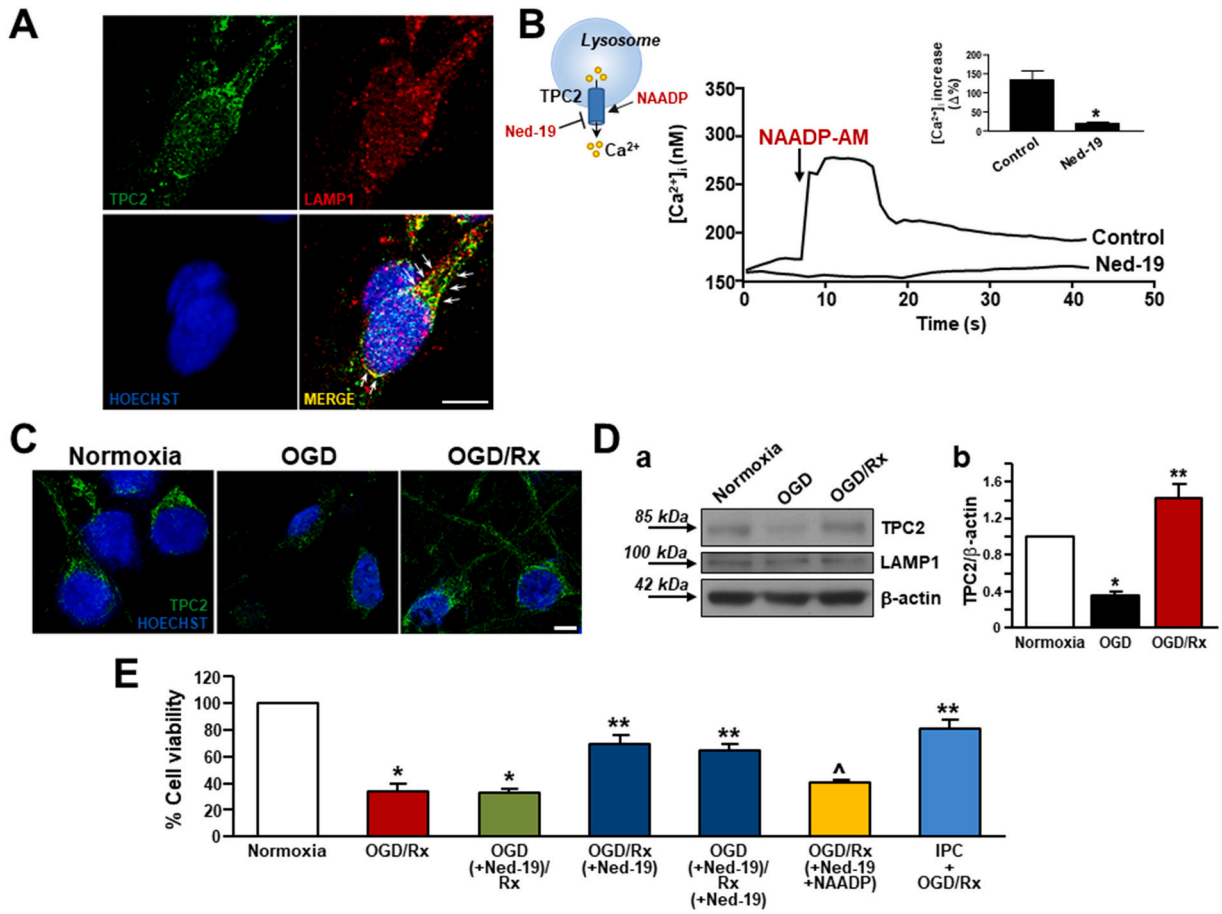

Fig. 1. TPC2 expression and activity in rat primary cortical neurons under physiological and hypoxic conditions.
A, TPC2 and LAMP1 immunosignals in rat primary cortical neurons (% co-localization 50 ± 2). Scale bar: 10 μm. B, Representative superimposed traces showing the effect of NAADP (1 μM) on $[Ca^{2+}]i$ in Fura-2 loaded primary cortical neurons in the presence or absence of Ned-19 (30 μM, added 5 min before recording). Inset: quantification of B. Each bar represents the mean ± S.E. (n = 30 cells for each group in three experimental sessions). *$p < 0.05$ vs Control. Cartoon: TPC2 pharmacological modulation by Ned-19. C, TPC2 and Hoechst 33342 immunosignals under Normoxia or OGD/Rx. Considering TPC2 fluorescence in normoxia as 100%, OGD was 48% ± 8 ($p < 0.05$ vs normoxia) while OGD/Rx was 94% ± 8. D, Representative Western blotting of TPC2 expression in neurons under Normoxia or exposed to OGD/Rx (a); Quantification of TPC2 protein expression (b). Each bar represents the mean ± SE of three experiments. *$p < 0.05$ vs Normoxia; **$p < 0.05$ vs OGD and Normoxia. **E**, Effect of Ned-19 (30 μM) on cell viability rate of primary cortical neurons exposed to OGD/Rx. Cell viability was measured by MTT assay. Data are expressed as mean ± SE of three different experimental sessions. *$p < 0.05$ vs Normoxia; **$p < 0.05$ vs OGD/Rx; ^$p < 0.05$ vs OGD/Rx(+Ned-19).

3.2. Pharmacological inhibition of TPC2 lysosomal channel on organellar calcium homeostasis, endoplasmic reticulum (ER) stress and autophagy

Endoplasmic reticulum (ER) stress, accompanied to organellar Ca^{2+} dysfunction, is now considered one of the main Stroke pathomechanisms (Sirabella et al., 2009; Secondo et al., 2019; Tedeschi et al., 2021). Of note, ER stress is linked to lysosomal homeostasis dysfunction during neurodegeneration (Tedeschi et al., 2019a, 2019b). Therefore, the impact of TPC2 inhibition on ER stress induction has been studied under hypoxic conditions. The addition of Ned-19 (30 μM) during the reoxygenation reverted the overexpression of the ER stress sensor, GRP78, and caspase 9 (Fig. 2A, a-c). As a functional correlate, ER Ca^{2+} level was measured indirectly as $[Ca^{2+}]_i$ increase triggered by blocking SERCA with thapsigargin (Fig. 2) revealing that Ned-19 hampered detrimental ER Ca^{2+} leak in hypoxic neurons, restoring organellar calcium homeostasis (Fig. 2B, a-c).

Due to the functional cooperation between ER and lysosomes in exchanging Ca^{2+} ions, membrane-permeable dipeptide GPN (300 μM) elicited a lower $[Ca^{2+}]_i$ increase in cortical neurons exposed to OGD + reoxygenation than in normoxic controls (Fig. 3A) thus unrevealing a detrimental reduction of lysosomal Ca^{2+} content. However, in the presence of Ned-19 (added at the onset of reoxygenation phase), GPN-elicited $[Ca^{2+}]_i$ increase was similar to that of normoxic controls (Fig. 3A), thus showing the acquisition of a prosurvival homeostatic change. The same results were mirrored by ML-SA1 (10 μM), another Ca^{2+} releasing agent specifically stimulating lysosomal TRPML1 channel (Fig. 3B).

Autophagy requires formation of a double-membrane structure containing the sequestered cytoplasmic material, the autophagosome, that ultimately fuses with the lysosome forming autolysosome. The addition of Ned-19 during the reoxygenation phase determined a sustained blocking effect on the autophagic flux. Consistently, this drug enhanced the expression of p62 and the lipidated form of LC3-I protein, LC3-II, in cortical neurons exposed to OGD + reoxygenation (Fig. 3C, a-d). Under hypoxic conditions, LAMP1 and LC3-II co-immunoprecipitation experiments (co-IP) revealed the ability of Ned-19 to interfere with the last phase of autophagy characterized by the fusion of autophagosome with lysosome (Fig. 3D). To corroborate these data, fluorescent signal intensity of autolysosomes was measured during OGD plus reoxygenation in the presence of Ned-19. Of note, TPC2 pharmacological inhibition with Ned-19 significantly reduced autolysosome formation in OGD plus reoxygenation compared with OGD plus reoxygenation alone (Fig. 3E) thus confirming LAMP1/LC3-II co-IP data (please see Fig. 3D). Since LC3-II is recruited to the autophagosomal membrane (Kabeya et al., 2000, 2004), our data might suggest that TPC2 blockade during OGD plus reoxygenation could interfere with the autophagic flux at the

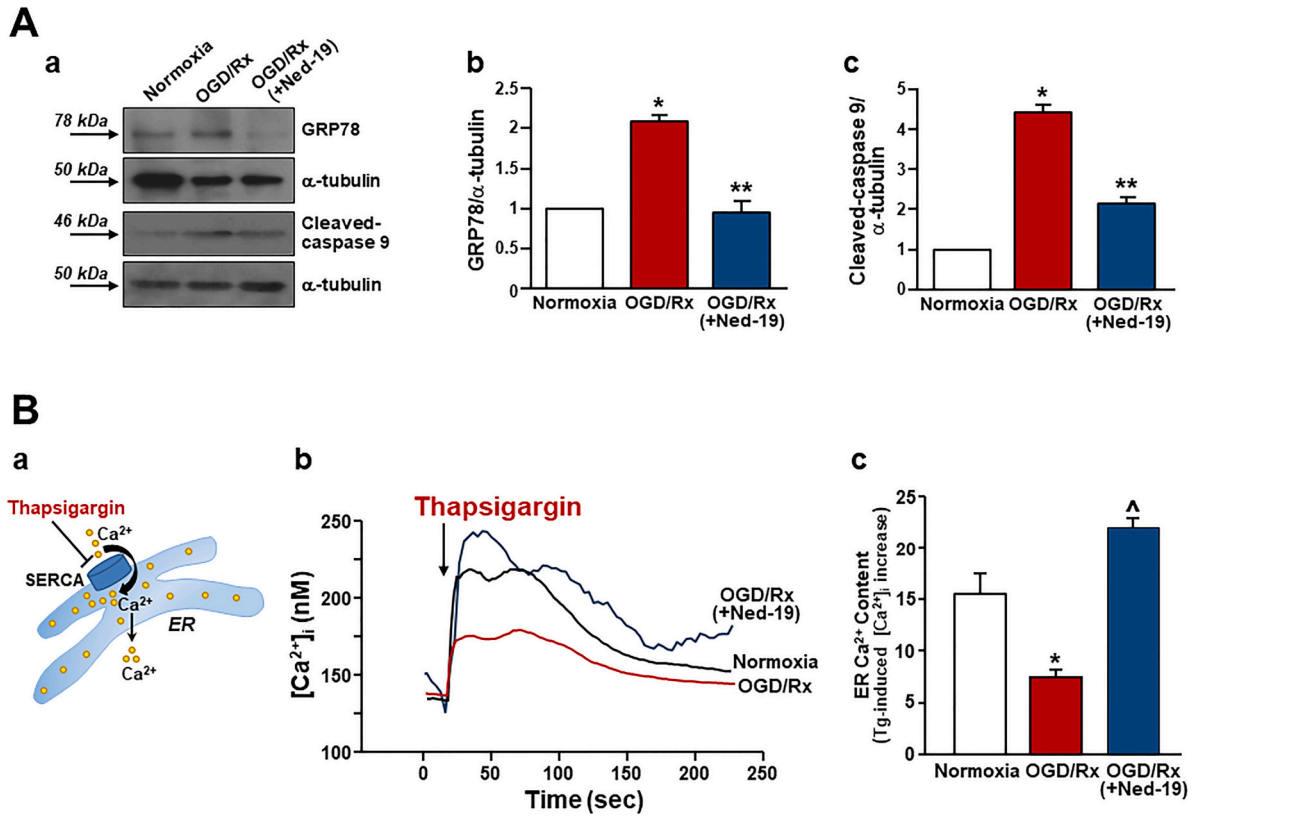

Fig. 2. TPC2 pharmacological inhibition by Ned-19 on ER Ca^{2+} content and ER stress in rat primary cortical neurons exposed to OGD + reoxygenation.
A, Representative Western blotting (a) and quantification (b, c) of GRP78 and cleaved caspase-9 expression under Normoxia or OGD/Rx in absence or presence of Ned-19 (added at the onset of reoxygenation). Each bar represents the mean ± SE of four experiments. * $p < 0.05$ vs Normoxia; ** $p < 0.05$ vs OGD/Rx. B, Cartoon of ER (a), superimposed traces (b) and quantification (c) of the effect of the SERCA inhibitor Thapsigargin on $[Ca^{2+}]_i$ under Normoxia or OGD/Rx in absence or presence of Ned-19 (added at the onset of reoxygenation). Thapsigargin (1 μM) was perfused in Normal Krebs solution (5.5 mM KCl, 160 mM NaCl, 1.2 mM $MgCl_2$, 1.5 mM $CaCl_2$, 10 mM glucose, and 10 mM HEPES-NaOH; pH 7.4). Experiments were repeated 3 times on 15 cells for Normoxia, 25 and 30 cells for OGD/Rx and OGD/Rx (+Ned-19), respectively. * $p < 0.05$ vs Normoxia, ^ $p < 0.05$ vs OGD/Rx.

level of the "fusion phase".

3.3. Effect of TPC2 knocking down on cell viability in primary hypoxic cortical neurons

To deepen the characterization of the role of TPC2 in hypoxic cortical neurons, this lysosomal channel was knocked down with two different siRNAs, alone or in combination, thus efficiently reducing channel expression (Fig. 4A) and function, as demonstrated by the prevention of NAADP-induced $[Ca^{2+}]_i$ increase (Fig. 4Ba,b). The entity of TPC2 functional inhibition by siRNAs was similar to that induced by pharmacological inhibition with Ned-19 (Fig. 4B,a,b). Consistently, siRNAs prevented the expression of TPC2 protein during the reoxygenation phase in hypoxic cortical neurons (Fig. 4C) as well as neuronal cytotoxicity (Fig. 4D).

3.4. Effect of pharmacological inhibition of TPC2 on brain infarct volume and neurological deficits of rats subjected to focal ischemia

To establish the effect of TPC2 pharmacological modulation in focal ischemia and to verify the dysfunction of the main autophagic markers, rats subjected to tMCAO were icv injected with Ned-19 at the onset of reperfusion at dosages of 20, 40 and 80-fold higher than the concentration used in vitro. Interestingly, Ned-19 treatment significantly reduced tMCAO-induced ischemic volume as well as tMCAO-induced neurological deficits compared with vehicle-treated animals (Fig. 5 A, B). However, at the highest dosage, Ned-19 failed to determine protection as well as prevention of general and focal deficits (Fig. 5). As demonstrated in hypoxic neurons, Ned-19 (40×) potentiated the increase of both p62 and LC3-II protein expression in the ipsilateral ischemic cortex compared with vehicle-treated ischemic animals (Fig. 6A-C) thus displaying a significant autophagy blockade.

4. Discussion

Our findings showed that the pharmacological blockade of TPC2 lysosomal channel by Ned-19 rescued primary cortical neurons from hypoxia-induced cell death and reduced the infarct volume in rats subjected to focal ischemia by hampering a hyperfunctional autophagic flux. Consistently, under ischemic conditions autophagy inhibition through TPC2 modulation should be considered a new therapeutic option (Liu and Levine, 2015). Indeed, in *post-mortem* human brain tissue from patients with a history of Stroke, abundant LC3-immunolabelled autophagic vacuoles have been found (Frugier et al., 2016). This evidence is suggestive of the concept that the 'load' of cellular debris and damaged proteins may trigger a hyperactivation of autophagy (Wen et al., 2008; Li et al., 2010; Shi et al., 2012). Furthermore, in cerebrospinal fluid (CSF) and serum of acute ischemic Stroke patients, autophagy markers such as Beclin-1 and LC3 are increased compared to control patients (Li et al., 2015), suggesting that autophagy is dramatically activated during Stroke. Of note, several studies suggest that, during cerebral ischemia, autophagy is predominantly a neuronal phenomenon (Carloni et al., 2008; Rami et al., 2008) in which the strict correlation among autophagic-lysosomal genes function, oxidative stress and excitotoxicity may influence the rate of the process (Yap et al., 2016).

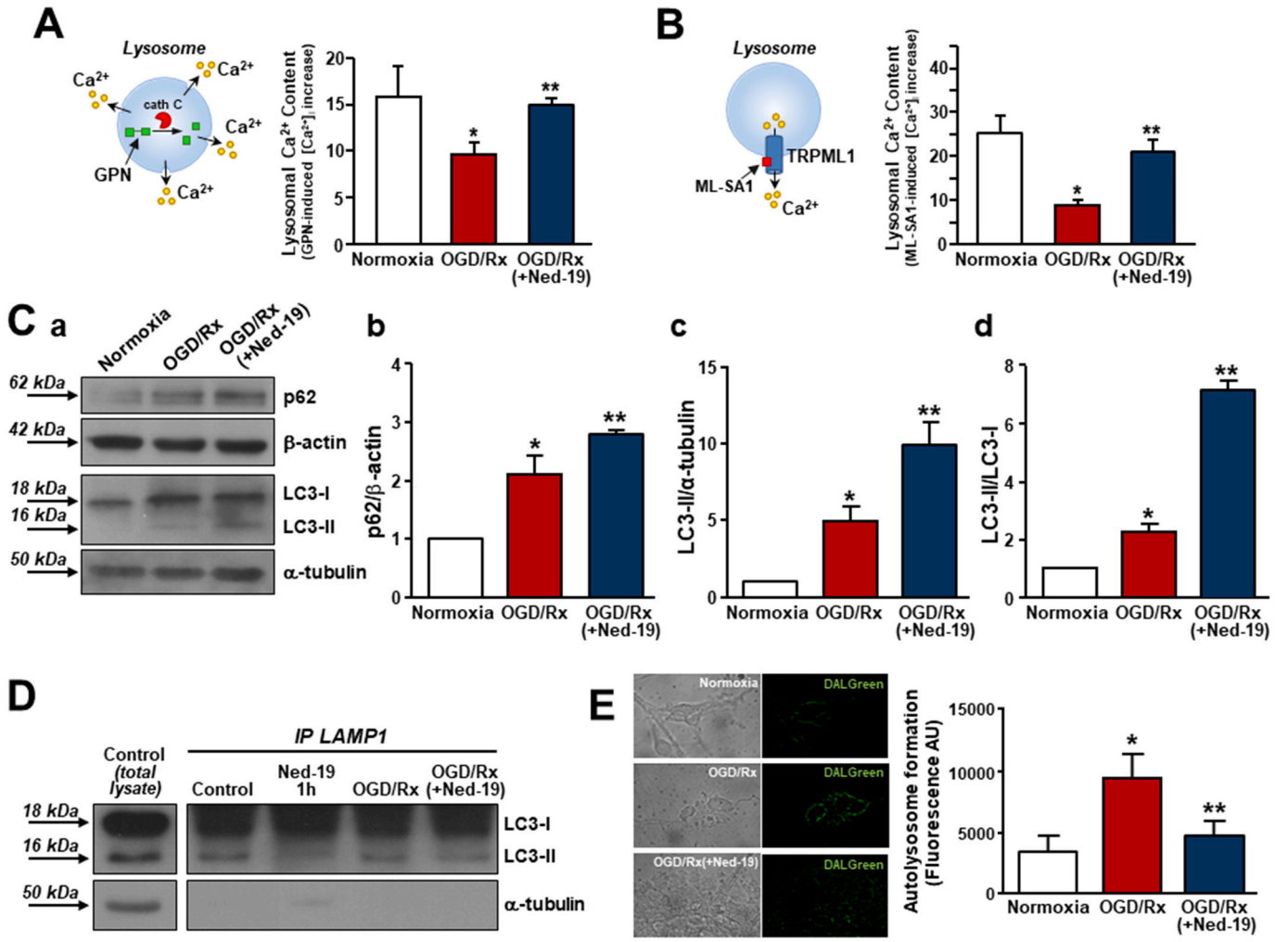

Fig. 3. TPC2 pharmacological inhibition by Ned-19 on lysosomal Ca^{2+} content and autophagy in rat primary cortical neurons exposed to OGD + reoxygenation. A, Cartoon of lysosomotrope agent GPN (300 μM) and quantification of its effect on lysosomal Ca^{2+} content under Normoxia or OGD/Rx in absence or presence of Ned-19 (added at the onset of reoxygenation). Experiments were repeated 3 times on 10 cells for Normoxia, 15 and 30 cells for OGD/Rx and OGD/Rx(+Ned-19), respectively. * $p < 0.05$ vs Normoxia, ** $p < 0.05$ vs OGD/Rx. B, Cartoon of lysosomal TRPML1 activation by ML-SA1 (10 μM) and quantification of its effect on lysosomal Ca^{2+} measured as $[Ca^{2+}]_i$ increase under Normoxia or OGD/Rx in absence or presence of Ned-19 (added at the onset of reoxygenation). Experiments were repeated 3 times on 30 cells for Normoxia, 30 and 35 cells for OGD/Rx and OGD/Rx(+Ned19), respectively. * $p < 0.05$ vs Normoxia, ** $p < 0.05$ vs OGD/Rx. C, Representative Western blotting (a) and quantification (b-d) of p62, and LC3 expression under Normoxia or OGD/Rx in absence or presence of Ned-19 (added at the onset of reoxygenation). Each bar represents the mean ± SE of four experiments. * $p < 0.05$ vs Normoxia; ** $p < 0.05$ vs OGD/Rx. D, LAMP1/LC3 immunoprecipitation (IP) using α-tubulin as loading control. Experiments were repeated 3 times on different neuronal preparations. E, Representative images of DAL-Green experiments (left) and quantification of autolysosome formation as arbitrary units in cortical neurons under normoxia, OGD plus reoxygenation and OGD plus reoxygenation + Ned-19 (right). *$p < 0.05$ vs normoxia; ** $p < 0.05$ vs OGD/Rx. (For interpretation of the references to colour in this figure legend, the reader is referred to the web version of this article.)

Moreover, autophagy is finely regulated by lysosomal function through the intervention of lysosomal Ca^{2+} channels able to modulate a specific transductional signaling pathway (Pereira et al., 2011; Medina et al., 2015). Being an efficient Ca^{2+} store dialoguing with other organelles including ER, lysosome regulates Ca^{2+} content of the main store through the control of ER Ca^{2+} releasing events (Tedeschi et al., 2021). The impairment of one of these two organelles negatively impacts the function of the other one thus triggering ER Ca^{2+} depletion and ER stress. Mechanistically, ER stress promotes the dissociation of the ER luminal calcium-binding chaperone GRP78 from the luminal site of the UPR transducers, thus activating their signaling. Since GRP78 has a high Ca^{2+} buffering capacity, dysregulation of ER/lysosome Ca^{2+} handling, due to the dysfunctional machinery of lysosome, may aggravate ER stress. Therefore, the neuroprotection exerted by Ned-19 in hypoxic neurons, by restoring lysosomal Ca^{2+} homeostasis, determined also the reduction of ER stress and GRP78 over-expression. Prevention of ER calcium loss reduces ER stress-dependent cell death under hypoxic conditions, a therapeutical strategy evoked for several neurological diseases including Stroke (Sirabella et al., 2009; Yap et al., 2016) and cardiac ischemia (Simon et al., 2021).

TPC2 pharmacological inhibition, equilibrating a correct neuronal organellar Ca^{2+} homeostasis, determined a large spectrum of protective effects under ischemic conditions. Consistently, the addition of Ned-19 during the reoxygenation phase not only prevented the overexpression of the ER stress sensor GRP78 but it hampered the death cascade head by caspase 9. This impressive effect is linked to the functional interplay between lysosome and ER in handling Ca^{2+} since Ned-19 prevented ER Ca^{2+} leak in primary cortical neurons exposed to OGD + reoxygenation.

However, the main result of the present study suggests that the blockade of autophagy during the reperfusion phase of focal ischemia may represent a new strategic therapy in Stroke. Accordingly, the abnormal formation of autophagosomes in ischemic areas (Zhang et al.,

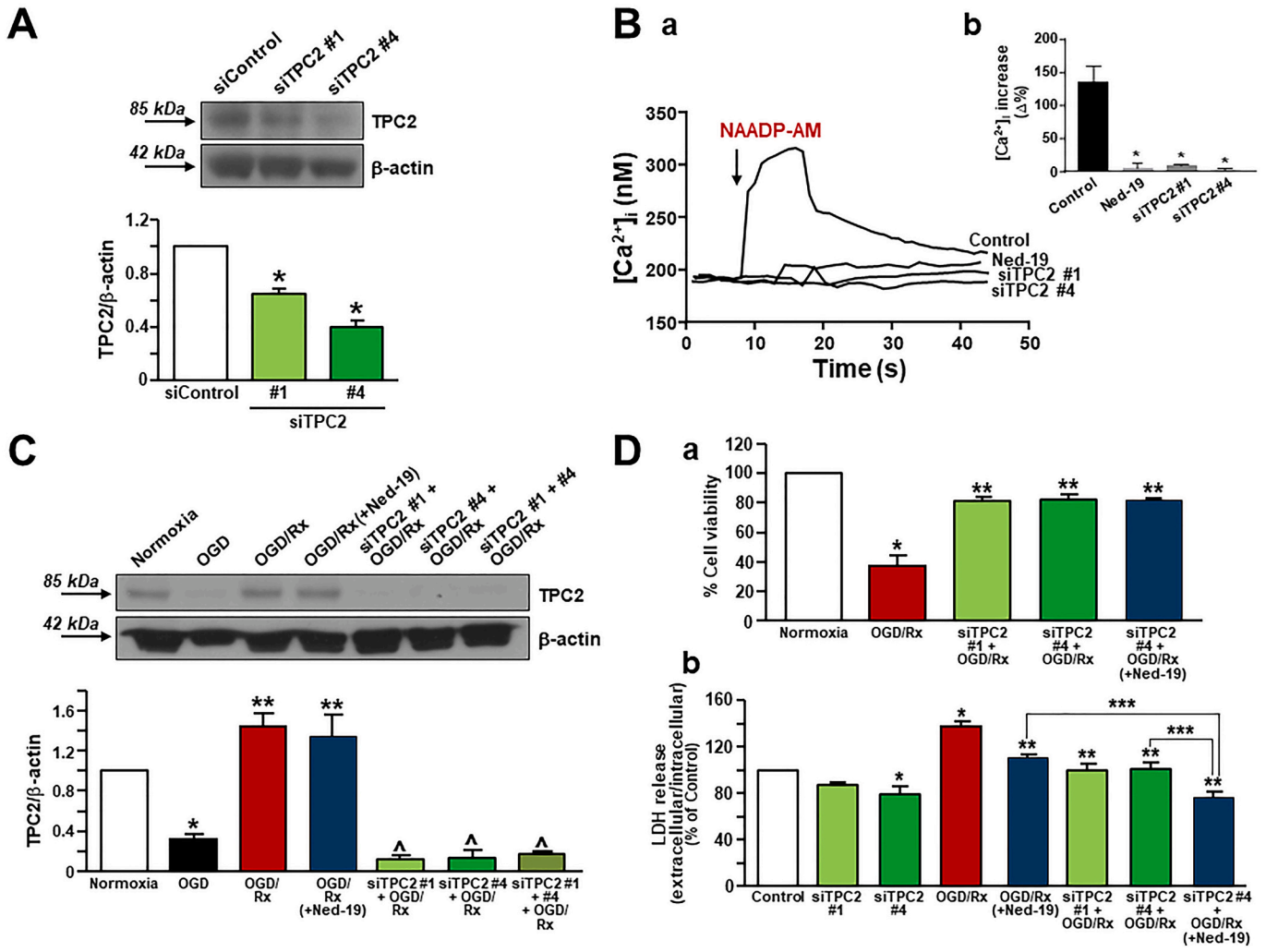

Fig. 4. TPC2 knocking down by siRNAs on cell death rate of rat primary cortical neurons exposed to OGD + reoxygenation.
A, Representative Western blotting and quantification of TPC2 expression in cortical neurons transfected with siControl or two different siRNAs against TPC2 channel (siTPC2s). Each bar represents the mean ± SE of three experiments. *p < 0.05 vs siControl. B, Representative superimposed traces showing the effect of the permeable form of NAADP (NAADP-AM, 1 μM) on $[Ca^{2+}]_i$ in Fura-2 loaded primary cortical neurons in the presence or absence of Ned-19 (30 μM), and after transfection with siTPC2s (a). Quantification of a (b). Each bar represents the mean ± S.E. ($n = 15$ cells for each group in three experimental sessions). *p < 0.05 vs Control. C, Representative Western blotting and quantification of TPC2 expression under Normoxia or OGD/Rx in absence or presence of siTPC2s. Each bar represents the mean ± SE of three experiments. *p < 0.05 vs Normoxia; **p < 0.05 vs OGD and Normoxia; ^p < 0.05 vs OGD/Rx alone or + Ned-19. D, Effect of siTPC2s on cell viability rate of primary cortical neurons exposed to OGD/Rx, measured by MTT assay in (a) and LDH release in (b). Data are expressed as mean ± S.E. of three different experimental sessions. *p < 0.05 vs Normoxia or Control; **p < 0.05 vs OGD/Rx; ***p < 0.05 vs OGD/Rx(+Ned-19) or siTPC2#4 + OGD/Rx.

2021) may affect glutamate clearance mechanism exacerbating the detrimental effect of excitotoxins (Katsumata et al., 2010). In this consideration, the hyperactivation of the autophagy flux is a plausible detrimental mechanism that contributes to further potentiate proteostatic imbalance and glutamate toxicity. However, we detected an initial mild autophagy blockade in neurons exposed to OGD + reoxygenation as a putative compensatory mechanism. Moreover, a further autophagy blockade induced by Ned-19 determined neuroprotection in focal ischemia, ascertained by p62 and LC3-II overexpression either in hypoxic neurons or in ipsilateral brain cortices from rats subjected to tMCAO+Ned-19. Specifically, TPC2 pharmacological inhibition interferes with autophagy at the level of the fusion phase hampering excessive autophagic flux. In this light, TPC2 inhibition may be useful to protect neurons from proteostasis dysfunction, ER stress and glutamate receptor-mediated excitotoxicity in a setting of a multi-target approach performed by a modulation of a single target. Considering that these multiple signaling pathways are interconnected, the present study identifies TPC2 lysosomal channel as a putative target possibly presiding this complex cascade providing an effective clinical management of Stroke.

Authors contributions

Conceptualization and Supervision: A.S.; Data Curation: V.T., M.J.S., A.V., A.S. and G.P.; Formal Analysis and Investigation: V.T., M.J.S., A.V.; Writing-Original Draft, and Review and Editing: A.S., G.P.; Funding Acquisition, A.S., V.T.

Funding

This work was supported by PRIN2015–Prot. 2015KRYSJN- from the Italian Ministry of Education and Research to A.S., Progetto Speciale di Ateneo (CA.04_CDA_n_103 27.03.2019 to A.S.), Progetto FRA (CdA_54_2020_FRA to A.S.) and Progetto Fondazione Roche per la Ricerca Indipendente 2021 (57254) to V.T.

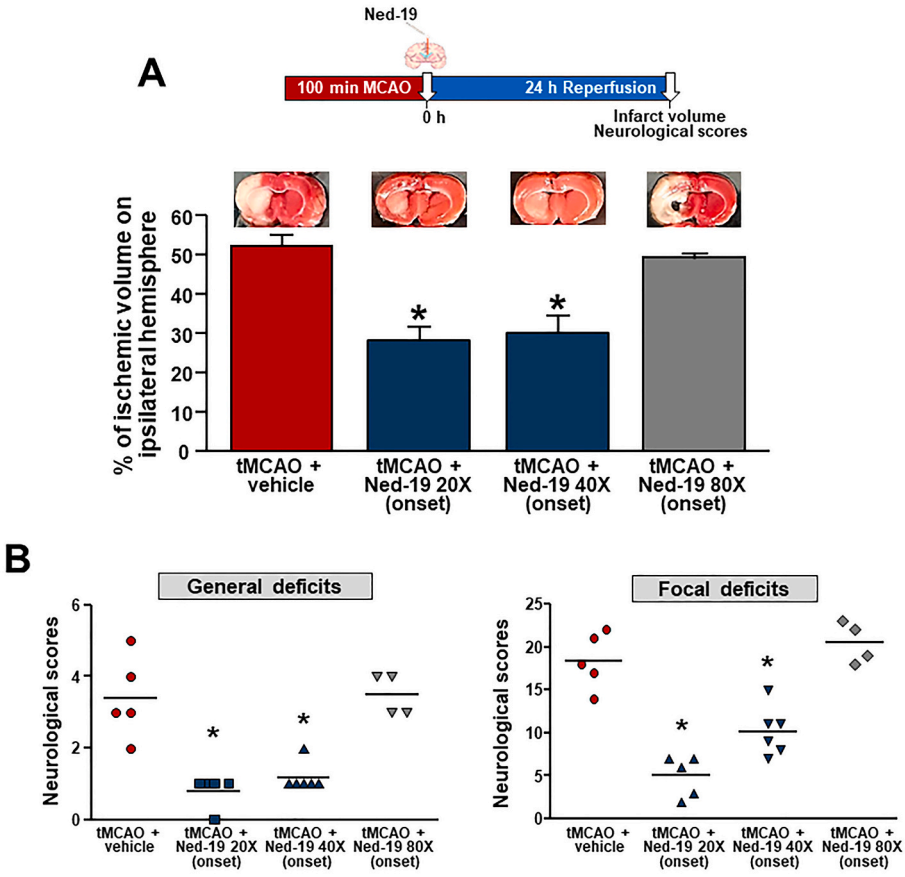

Fig. 5. TPC2 pharmacological inhibition by Ned-19 on infarct volume and neurological deficits of rats subjected to tMCAO.
A, Infarct volume in rats subjected to tMCAO+vehicle and tMCAO+Ned-19 at different dosages ($N = 8$ animals for each group). Each column represents the percent ratio between the volumes of the hemispheres ipsi- and contralateral to tMCAO in each group. No ischemic damage was detected in sham-operated animals. Mice were euthanized 24 h after surgery. *$p < 0.05$ vs tMCAO+vehicle. B, Neurological deficits (general and focal) in rats subjected to the treatments in A. *$p < 0.05$ vs each respective "tMCAO+vehicle".

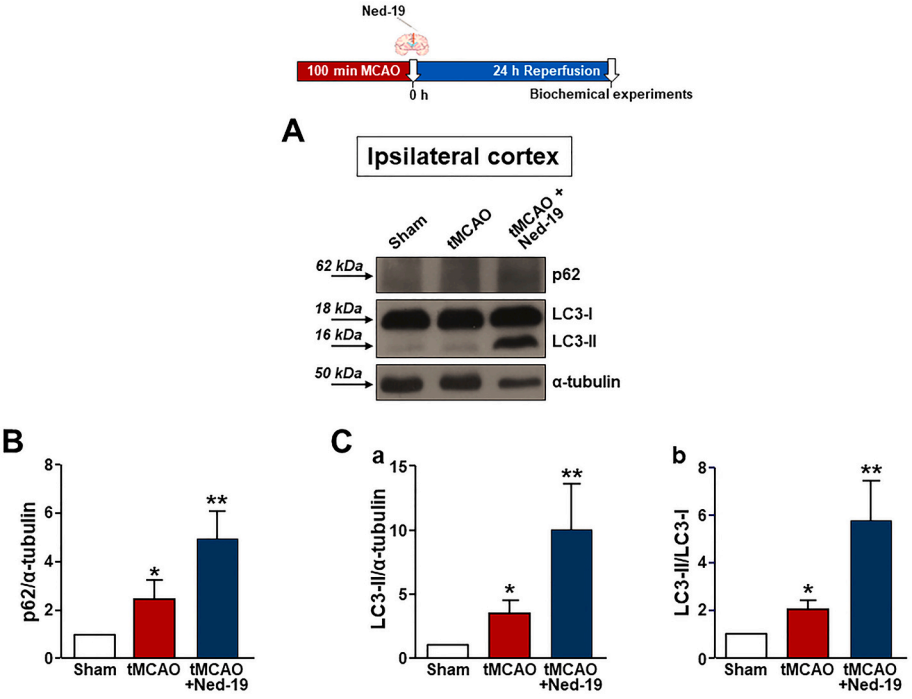

Fig. 6. TPC2 pharmacological inhibition by Ned-19 on autophagy markers expression in ipsilateral cortices of rats subjected to tMCAO.
A-C, Representative Western blotting (A) and quantification (B, C) of p62, and LC3 expression in ipsilateral cortices of sham-operated and ischemic rats. Values are expressed as mean ± S.E. Experiments were repeated 3 times on different brain preparations. *$p < 0.05$ vs each respective Sham; **$p < 0.05$ vs each respective tMCAO.

Disclosures

None.

Data availability

Data will be made available on request.

Appendix A. Supplementary data

Supplementary data to this article can be found online at https://doi.org/10.1016/j.nbd.2023.106020.

References

Bae, M., Patel, N., Xu, H., Lee, M., Tominaga-Yamanaka, K., Nath, A., Geiger, J., Gorospe, M., Mattson, M.P., Haughey, N.J., 2014. Activation of TRPML1 clears intraneuronal Aβ in preclinical models of HIV infection. J. Neurosci. 34, 11485–11503. https://doi.org/10.1523/JNEUROSCI.0210-14.2014.

Bederson, J.B., Pitts, L.H., Germano, S.M., Nishimura, M.C., Davis, R.L., Bartkowski, H. M., 1986. Evaluation of 2,3,5-triphenyltetrazolium chloride as a stain for detection and quantification of experimental cerebral infarction in rats. Stroke 17, 1304–1308. https://doi.org/10.1161/01.str.17.6.1304.

Boccaccio, A., Scholz-Starke, J., Hamamoto, S., Larisch, N., Festa, M., Gutla, P.V., Costa, A., Dietrich, P., Uozumi, N., Carpaneto, A., 2014. The phosphoinositide PI (3,5)P_2 mediates activation of mammalian but not plant TPC proteins: functional expression of endolysosomal channels in yeast and plant cells. Cell. Mol. Life Sci. 71, 4275–4283. https://doi.org/10.1007/s00018-014-1623-2.

Brailoiu, E., Churamani, D., Pandey, V., Brailoiu, G.C., Tuluc, F., Patel, S., Dun, N.J., 2006. Messenger-specific role for nicotinic acid adenine dinucleotide phosphate in neuronal differentiation. J. Biol. Chem. 281, 15923–15928. https://doi.org/10.1074/jbc.M602249200.

Brailoiu, E., Churamani, D., Cai, X., Schrlau, M.G., Brailoiu, G.C., Gao, X., Hooper, R., Boulware, M.J., Dun, N.J., Marchant, J.S., Patel, S., 2009. Essential requirement for two-pore channel 1 in NAADP-mediated calcium signaling. J. Cell Biol. 186, 201–209. https://doi.org/10.1083/jcb.200904073.

Brailoiu, E., Rahman, T., Churamani, D., Prole, D.L., Brailoiu, G.C., Hooper, R., Taylor, C. W., Patel, S., 2010. An NAADP-gated two-pore channel targeted to the plasma membrane uncouples triggering from amplifying Ca^{2+} signals. J. Biol. Chem. 285, 38511–38516. https://doi.org/10.1074/jbc.M110.162073.

Calcraft, P.J., Ruas, M., Pan, Z., Cheng, X., Arredouani, A., Hao, X., Tang, J., Rietdorf, K., Teboul, L., Chuang, K.T., Lin, P., Xiao, R., Wang, C., Zhu, Y., Lin, Y., Wyatt, C.N., Parrington, J., Ma, J., Evans, A.M., Galione, A., Zhu, M.X., 2009. NAADP mobilizes calcium from acidic organelles through two-pore channels. Nature 459, 596–600. https://doi.org/10.1038/nature08030.

Cang, C., Bekele, B., Ren, D., 2014. The voltage-gated sodium channel TPC1 confers endolysosomal excitability. Nat. Chem. Biol. 10, 463–469. https://doi.org/10.1038/nchembio.1522.

Carloni, S., Buonocore, G., Balduini, W., 2008. Protective role of autophagy in neonatal hypoxia-ischemia induced brain injury. Neurobiol. Dis. 32, 329–339. https://doi.org/10.1016/j.nbd.2008.07.022.

Colacurcio, D.J., Nixon, R.A., 2016. Disorders of lysosomal acidification-the emerging role of v-ATPase in aging and neurodegenerative disease. Ageing Res. Rev. 32, 75–88. https://doi.org/10.1016/j.arr.2016.05.004.

Foster, W.J., Taylor, H.B.C., Padamsey, Z., Jeans, A.F., Galione, A., Emptage, N.J., 2018. Hippocampal mGluR1-dependent long-term potentiation requires NAADP-mediated acidic store Ca^{2+} signaling. Sci. Signal. 11, eaat9093. https://doi.org/10.3389/fcell.2020.00496.

Frugier, T., Taylor, J.M., McLean, C., Bye, N., Beart, P.M., Devenish, R.J., Crack, P.J., 2016. Evidence for the recruitment of autophagic vesicles in human brain after stroke. Neurochem. Int. 96, 62–68. https://doi.org/10.1016/j.neuint.2016.02.016.

García-Rúa, V., Feijóo-Bandín, S., Rodríguez-Penas, D., Mosquera-Leal, A., Abu-Assi, E., Beiras, A., María Seoane, L., Lear, P., Parrington, J., Portolés, M., Roselló-Lletí, E., Rivera, M., Gualillo, O., Parra, V., Hill, J.A., Rothermel, B., González-Juanatey, J.R., Lago, F., 2016. Endolysosomal two-pore channels regulate autophagy in cardiomyocytes. J. Physiol. 594, 3061–3077. https://doi.org/10.1113/JP271332.

Grimm, C., Holdt, L.M., Chen, C.C., Hassan, S., Müller, C., Jörs, S., Cuny, H., Kissing, S., Schröder, B., Butz, E., Northoff, B., Castonguay, J., Luber, C.A., Moser, M., Spahn, S., Lüllmann-Rauch, R., Fendel, C., Klugbauer, N., Griesbeck, O., Haas, A., Mann, M., Bracher, F., Teupser, D., Saftig, P., Biel, M., Wahl-Schott, C., 2014. High susceptibility to fatty liver disease in two-pore channel 2-deficient mice. Nat. Commun. 5, 4699. https://doi.org/10.1038/ncomms5699.

Grynkiewicz, G., Poenie, M., Tsien, R.Y., 1985. A new generation of Ca^{2+} indicators with greatly improved fluorescence properties. J. Biol. Chem. 260, 3440–3450. https://doi.org/10.1016/S0021-9258(19)83641-4.

Guo, J., Zeng, W., Jiang, Y., 2017. Tuning the ion selectivity of two-pore channels. Proc. Natl. Acad. Sci. U. S. A. 114, 1009–1014. https://doi.org/10.1073/pnas.1616191114.

Guo, C., Webb, S.E., Chan, C.M., Miller, A.L., 2020. TPC2-mediated Ca^{2+} signaling is required for axon extension in caudal primary motor neurons in zebrafish embryos. J. Cell Sci. 133, jcs244780. https://doi.org/10.1242/jcs.244780.

Hermann, J., Bender, M., Schumacher, D., Woo, M.S., Shaposhnykov, A., Rosenkranz, S. C., Kuryshev, V., Meier, C., Guse, A.H., Friese, M.A., Freichel, M., Tsvilovskyy, V., 2020. Contribution of NAADP to glutamate-evoked changes in Ca^{2+} homeostasis in mouse hippocampal neurons. Front. Cell Dev. Biol. 8, 496. https://doi.org/10.3389/fcell.2020.00496.

Hou, K., Xu, D., Li, F., Chen, S., Li, Y., 2019. The progress of neuronal autophagy in cerebral ischemia stroke: mechanisms, roles and research methods. J. Neurol. Sci. 400, 72–82. https://doi.org/10.1016/j.jns.2019.03.015.

Kabeya, Y., Mizushima, N., Ueno, T., Yamamoto, A., Kirisako, T., Noda, T., Kominami, E., Ohsumi, Y., Yoshimori, T., 2000. LC3, a mammalian homologue of yeast Apg8p, is localized in autophagosome membranes after processing. EMBO J. 19, 5720–5728. https://doi.org/10.1093/emboj/19.21.5720.

Kabeya, Y., Mizushima, N., Yamamoto, A., Oshitani-Okamoto, S., Ohsumi, Y., Yoshimori, T., 2004. LC3, GABARAP and GATE16 localize to autophagosomal membrane depending on form-II formation. J. Cell Sci. 117, 2805–2812. https://doi.org/10.1242/jcs.01131.

Katsumata, K., Nishiyama, J., Inoue, T., Mizushima, N., Takeda, J., Yuzaki, M., 2010. Dynein- and activity-dependent retrograde transport of autophagosomes in neuronal axons. Autophagy 6, 378–385. https://doi.org/10.4161/auto.6.3.11262.

Li, Q., Li, H., Roughton, K., Wang, X., Kroemer, G., Blomgren, K., Zhu, C., 2010. Lithium reduces apoptosis and autophagy after neonatal hypoxia-ischemia. Cell Death Dis. 1, e56 https://doi.org/10.1038/cddis.2010.33.

Li, Q., Zhang, T., Wang, J., Zhang, Z., Zhai, Y., Yang, G.Y., Sun, X., 2014. Rapamycin attenuates mitochondrial dysfunction via activation of mitophagy in experimental ischemic stroke. Biochem. Biophys. Res. Commun. 444, 182–188. https://doi.org/10.1016/j.bbrc.2014.01.032.

Li, H., Qiu, S., Li, X., Li, M., Peng, Y., 2015. Autophagy biomarkers in CSF correlates with infarct size, clinical severity and neurological outcome in AIS patients. J. Transl. Med. 13, 359. https://doi.org/10.1186/s12967-015-0726-3.

Liu, Y., Levine, B., 2015. Autosis and autophagic cell death: the dark side of autophagy. Cell Death Differ. 22, 367–376. https://doi.org/10.1038/cdd.2014.143.

Medina, D.L., 2021. Lysosomal calcium and autophagy. Int. Rev. Cell Mol. Biol. 362, 141–170. https://doi.org/10.1016/bs.ircmb.2021.03.002.

Medina, D.L., Di Paola, S., Peluso, I., Armani, A., De Stefani, D., Venditti, R., Montefusco, S., Scotto-Rosato, A., Prezioso, C., Forrester, A., Settembre, C., Wang, W., Gao, Q., Xu, H., Sandri, M., Rizzuto, R., De Matteis, M.A., Ballabio, A., 2015. Lysosomal calcium signalling regulates autophagy through calcineurin and TFEB. Nat. Cell Biol. 17, 288–299. https://doi.org/10.1038/ncb3114.

Nixon, R.A., 2013. The role of autophagy in neurodegenerative disease. Nat. Med. 19, 983–997. https://doi.org/10.1038/nm.3232.

Patel, S., 2015. Function and dysfunction of two-pore channels. Sci. Signal. 8, re7. https://doi.org/10.1126/scisignal.aab3314.

Patel, S., Kilpatrick, B.S., 2018. Two-pore channels and disease. Biochim. Biophys. Acta, Mol. Cell Res. 1865, 1678–1686. https://doi.org/10.1016/j.bbamcr.2018.05.004.

Pereira, G.J., Hirata, H., Fimia, G.M., do Carmo, L.G., Bincoletto, C., Han, S.W., Stilhano, R.S., Ureshino, R.P., Bloor-Young, D., Churchill, G., Piacentini, M., Patel, S., Smaili, S.S., 2011. Nicotinic acid adenine dinucleotide phosphate (NAADP) regulates autophagy in cultured astrocytes. J. Biol. Chem. 286, 27875–27881. https://doi.org/10.1074/jbc.C110.216580.

Pereira, G.J., Antonioli, M., Hirata, H., Ureshino, R.P., Nascimento, A.R., Bincoletto, C., Vescovo, T., Piacentini, M., Fimia, G.M., Smaili, S.S., 2017. Glutamate induces autophagy via the two-pore channels in neural cells. Oncotarget 8, 12730–12740. https://doi.org/10.18632/oncotarget.14404.

Pitt, S.J., Funnell, T.M., Sitsapesan, M., Venturi, E., Rietdorf, K., Ruas, M., Ganesan, A., Gosain, R., Churchill, G.C., Zhu, M.X., Parrington, J., Galione, A., Sitsapesan, R., 2010. TPC2 is a novel NAADP-sensitive Ca^{2+} release channel, operating as a dual sensor of luminal pH and Ca^{2+}. J. Biol. Chem. 285, 35039–35046. https://doi.org/10.1074/jbc.M110.156927.

Rami, A., Langhagen, A., Steiger, S., 2008. Focal cerebral ischemia induces upregulation of Beclin 1 and autophagy-like cell death. Neurobiol. Dis. 29, 132–141. https://doi.org/10.1016/j.nbd.2007.08.005.

Ruas, M., Rietdorf, K., Arredouani, A., Davis, L.C., Lloyd-Evans, E., Koegel, H., Funnell, T. M., Morgan, A.J., Ward, J.A., Watanabe, K., Cheng, X., Churchill, G.C., Zhu, M.X., Platt, F.M., Wessel, G.M., Parrington, J., Galione, A., 2010. Purified TPC isoforms form NAADP receptors with distinct roles for ca(2+) signaling and endolysosomal trafficking. Curr. Biol. 20, 703–709. https://doi.org/10.1016/j.cub.2010.02.049.

Ruas, M., Davis, L.C., Chen, C.C., Morgan, A.J., Chuang, K.T., Walseth, T.F., Grimm, C., Garnham, C., Powell, T., Platt, N., Biel, M., Wahl-Schott, C., Parrington, J., Galione, A., 2015. Expression of Ca^{2+}-permeable two-pore channels rescues NAADP signalling in TPC-deficient cells. EMBO J. 34, 1743–1758. https://doi.org/10.15252/embj.201490009.

Sakurai, Y., Kolokoltsov, A.A., Chen, C.C., Tidwell, M.W., Bauta, W.E., Klugbauer, N., Grimm, C., Wahl-Schott, C., Biel, M., Davey, R.A., 2015. Ebola virus. Two-pore channels control Ebola virus host cell entry and are drug targets for disease treatment. Science 347, 995–998. https://doi.org/10.1126/science.1258758.

Santoni, G., Maggi, F., Amantini, C., Marinelli, O., Nabissi, M., Morelli, M.B., 2020. Pathophysiological role of transient receptor potential Mucolipin Channel 1 in calcium-mediated stress-induced neurodegenerative diseases. Front. Physiol. 11, 251. https://doi.org/10.3389/fphys.2020.00251.

Schieder, M., Rötzer, K., Brüggemann, A., Biel, M., Wahl-Schott, C.A., 2010. Characterization of two-pore channel 2 (TPCN2)-mediated Ca^{2+} currents in isolated lysosomes. J. Biol. Chem. 285, 21219–21222. https://doi.org/10.1074/jbc.C110.143123.

Scorziello, A., Savoia, C., Sisalli, M.J., Adornetto, A., Secondo, A., Boscia, F., Esposito, A., Polishchuk, E.V., Polishchuk, R.S., Molinaro, P., Carlucci, A., Lignitto, L., Di Renzo, G., Feliciello, A., Annunziato, L., 2013. NCX3 regulates mitochondrial ca(2+)

handling though the AKAP121-anchored signaling complex and prevents hypoxia-induced neuronal death. J. Cell Sci. 126, 5566–5577. https://doi.org/10.1242/jcs.129668.

Secondo, A., Staiano, R.I., Scorziello, A., Sirabella, R., Boscia, F., Adornetto, A., Valsecchi, V., Molinaro, P., Canzoniero, L.M., Di Renzo, G., Di Renzo, G., Annunziato, L., 2007. BHK cells transfected with NCX3 are more resistant to hypoxia followed by reoxygenation than those transfected with NCX1 and NCX2: possible relationship with mitochondrial membrane potential. Cell Calcium 42, 521–535. https://doi.org/10.1016/j.ceca.2007.01.006.

Secondo, A., Petrozziello, T., Tedeschi, V., Boscia, F., Vinciguerra, A., Ciccone, R., Pannaccione, A., Molinaro, P., Pignataro, G., Annunziato, L., 2019. ORAI1/STIM1 interaction intervenes in stroke and in neuroprotection induced by ischemic preconditioning through store-operated calcium entry. Stroke 50, 1240–1249. https://doi.org/10.1161/STROKEAHA.118.024115.

She, J., Guo, J., Chen, Q., Zeng, W., Jiang, Y., Bai, X.C., 2018. Structural insights into the voltage and phospholipid activation of the mammalian TPC1 channel. Nature 556, 130–134. https://doi.org/10.1038/nature26139.

Shi, R., Weng, J., Zhao, L., Li, X.M., Gao, T.M., Kong, J., 2012. Excessive autophagy contributes to neuron death in cerebral ischemia. CNS Neurosci. Ther. 18, 250–260. https://doi.org/10.1111/j.1755-5949.2012.00295.x.

Simon, J.N., Vrellaku, B., Monterisi, S., Chu, S.M., Rawlings, N., Lomas, O., Marchal, G. A., Waithe, D., Syeda, F., Gajendragadkar, P.R., Jayaram, R., Sayeed, R., Channon, K. M., Fabritz, L., Swietach, P., Zaccolo, M., Eaton, P., Casadei, B., 2021. Oxidation of protein kinase a regulatory subunit PKARIα protects against myocardial ischemia-reperfusion injury by inhibiting lysosomal-triggered calcium release. Circulation 143, 449–465. https://doi.org/10.1161/CIRCULATIONAHA.120.046761.

Sirabella, R., Secondo, A., Pannaccione, A., Scorziello, A., Valsecchi, V., Adornetto, A., Bilo, L., Di Renzo, G., Annunziato, A., 2009. Anoxia-induced NF-kappaB-dependent upregulation of NCX1 contributes to Ca^{2+} refilling into endoplasmic reticulum in cortical neurons. Stroke 40, 922–929. https://doi.org/10.1161/STROKEAHA.108.531962.

Sisalli, M.J., Secondo, A., Esposito, A., Valsecchi, V., Savoia, C., Di Renzo, G.F., Annunziato, L., Scorziello, A., 2014. Endoplasmic reticulum refilling and mitochondrial calcium extrusion promoted in neurons by NCX1 and NCX3 in ischemic preconditioning are determinant for neuroprotection. Cell Death Differ. 21, 1142–1149. https://doi.org/10.1038/cdd.2014.32.

Tedeschi, V., Petrozziello, T., Secondo, A., 2019a. Calcium Dyshomeostasis and lysosomal Ca^{2+} dysfunction in amyotrophic lateral sclerosis. Cells 8, 1216. https://doi.org/10.3390/cells8101216.

Tedeschi, V., Petrozziello, T., Sisalli, M.J., Boscia, F., Canzoniero, L.M.T., Secondo, A., 2019b. The activation of Mucolipin TRP channel 1 (TRPML1) protects motor neurons from L-BMAA neurotoxicity by promoting autophagic clearance. Sci. Rep. 9, 10743. https://doi.org/10.1038/s41598-019-46708-5.

Tedeschi, V., Sisalli, M.J., Petrozziello, T., Canzoniero, L.M.T., Secondo, A., 2021. Lysosomal calcium is modulated by STIM1/TRPML1 interaction which participates to neuronal survival during ischemic preconditioning. FASEB J. 35, e21277 https://doi.org/10.1096/fj.202001886R.

Tsunemi, T., Perez-Rosello, T., Ishiguro, Y., Yoroisaka, A., Jeon, S., Hamada, K., Rammonhan, M., Wong, Y.C., Xie, Z., Akamatsu, W., Mazzulli, J.R., Surmeier, D.J., Hattori, N., Krainc, D., 2019. Increased lysosomal exocytosis induced by lysosomal Ca^{2+} channel agonists protects human dopaminergic neurons from α-Synuclein toxicity. J. Neurosci. 39, 5760–5772. https://doi.org/10.1523/JNEUROSCI.3085-18.2019.

Udayar, V., Chen, Y., Sidransky, E., Jagasia, R., 2022. Lysosomal dysfunction in neurodegeneration: emerging concepts and methods. Trends Neurosci. 45, 184–199. https://doi.org/10.1016/j.tins.2021.12.004.

Urbanczyk, J., Chernysh, O., Condrescu, M., Reeves, J.P., 2006. Sodium-calcium exchange does not require allosteric calcium activation at high cytosolic sodium concentrations. J. Physiol. 575, 693–705. https://doi.org/10.1113/jphysiol.2006.113910.

Vinciguerra, A., Formisano, L., Cerullo, P., Guida, N., Cuomo, O., Esposito, A., Di Renzo, G., Annunziato, L., Pignataro, G., 2014. MicroRNA-103-1 selectively downregulates brain NCX1 and its inhibition by anti-miRNA ameliorates stroke damage and neurological deficits. Mol. Ther. 22, 1829–1838. https://doi.org/10.1038/mt.2014.113.

Wang, X., Zhang, X., Dong, X.P., Samie, M., Li, X., Cheng, X., Goschka, A., Shen, D., Zhou, Y., Harlow, J., Zhu, M.X., Clapham, D.E., Ren, D., Xu, H., 2012. TPC proteins are phosphoinositide- activated sodium-selective ion channels in endosomes and lysosomes. Cell 151, 372–383. https://doi.org/10.1016/j.cell.2012.08.036.

Wen, Y.D., Sheng, R., Zhang, L.S., Han, R., Zhang, X., Zhang, X.D., Han, F., Fukunaga, K., Qin, Z.H., 2008. Neuronal injury in rat model of permanent focal cerebral ischemia is associated with activation of autophagic and lysosomal pathways. Autophagy 4, 762–769. https://doi.org/10.4161/auto.6412.

Yap, Y.W., Llanos, R.M., La Fontaine, S., Cater, M.A., Beart, P.M., Cheung, N.S., 2016. Comparative microarray analysis identifies commonalities in neuronal injury: evidence for oxidative stress, dysfunction of calcium Signalling, and inhibition of autophagy-lysosomal pathway. Neurochem. Res. 41, 554–567. https://doi.org/10.1007/s11064-015-1666-2.

Yu, S., Zheng, S., Leng, J., Wang, S., Zhao, T., Liu, J., 2016. Inhibition of mitochondrial calcium uniporter protects neurocytes from ischemia/reperfusion injury via the inhibition of excessive mitophagy. Neurosci. Lett. 628, 24–29. https://doi.org/10.1016/j.neulet.2016.06.012.

Zhang, Z.H., Lu, Y.Y., Yue, J., 2013. Two pore channel 2 differentially modulates neural differentiation of mouse embryonic stem cells. PLoS One 8, e66077. https://doi.org/10.1371/journal.pone.0066077.

Zhang, L., Fang, Y., Cheng, X., Lian, Y., Xu, H., Zeng, Z., Zhu, H., 2017. TRPML1 participates in the progression of Alzheimer's disease by regulating the PPARγ/AMPK/Mtor Signalling pathway. Cell. Physiol. Biochem. 43, 2446–2456. https://doi.org/10.1159/000484449.

Zhang, M., Lu, H., Xie, X., Shen, H., Li, X., Zhang, Y., Wu, J., Ni, J., Li, H., Chen, G., 2020. TMEM175 mediates lysosomal function and participates in neuronal injury induced by cerebral ischemia-reperfusion. Mol. Brain. 13, 113. https://doi.org/10.1186/s13041-020-00651-z.

Zhang, X., Wei, M., Fan, J., Yan, W., Zha, X., Song, H., Wan, R., Yin, Y., Wang, W., 2021. Ischemia-induced upregulation of autophagy preludes dysfunctional lysosomal storage and associated synaptic impairments in neurons. Autophagy 17, 1519–1542. https://doi.org/10.1080/15548627.2020.1840796.

Zuo, W., Zhang, S., Xia, C.Y., Guo, X.F., He, W.B., Chen, N.H., 2014. Mitochondria autophagy is induced after hypoxic/ischemic stress in a Drp1 dependent manner: the role of inhibition of Drp1 in ischemic brain damage. Neuropharmacology 86, 103–115. https://doi.org/10.1016/j.neuropharm.2014.07.002.